

# Demand Response Control for PHEV Charging Stations by Dynamic Price Adjustments

Daehyun Ban\*, George Michailidis<sup>†</sup>, and Michael Devetsikiotis\*

\*Department of Electrical and Computer Engineering, NC State University, Raleigh, NC 27695-7911

<sup>†</sup>Department of Statistics, University of Michigan, Ann Arbor, MI 48109-1092

dban@ncsu.edu, gmichail@umich.edu, mdevets@ncsu.edu

**Abstract**—Because of their economical operation and low environmental pollution, PHEVs (Plug-in Hybrid Electric Vehicles) are rapidly substituting gasoline vehicles. However, there still exist obstacles to proliferating their use, such as their relatively short driving range and long battery charging time. At the same time, it is recognized that the current increasing trend of PHEV use will have a serious impact on the stability of power grids (i.e., electricity providers). Along with improving the performance of PHEVs, the installation of charging stations, which addresses such problems, is essentially required in smart grid communities.

This paper proposes an operational framework for multiple PHEV charging stations. To maintain the power grid stability, regulating electric supply for charging stations through support planning is an attractive approach. In this direction, we determine a condition under which customers can receive improved QoS (Quality of Service), and provide an algorithm which allocates PHEVs into the condition.

Our analysis is based on a multi-queue system, used as a model of charging stations whose dynamics we investigate. Specifically, our interest is the performance change when demand responses (i.e., the behavior of customers) are controlled. We proceed with our investigation in two steps: In the first step, we consider the PHEV allocation problem. We formulate an optimization problem which can minimize the waiting time of customers and obtain its solution. Then, we additionally regard the size constraint of charging stations and propose an optimal PHEV allocation algorithm. In the second step, we modify this algorithm to work in realistic scenarios. If PHEVs do not receive any incentives (or penalties), there is no restriction to control their allocation. At the station side, we suggest price control methods and show that the optimal allocation can be attained by them. For each step, we provide test results to validate our analysis.

## I. INTRODUCTION

Increasing gasoline prices and environmental pollution make Plug-in Hybrid Electric Vehicles (PHEVs) more effective transportation option. Indeed, their use is rapidly penetrating in the market. The number of consumers who purchase a PHEV has been growing by 80% each year since 2000 [1] and 10% of new vehicle sales are expected to be PHEVs by year 2015 [2].

However, there still exist obstacles to the proliferation of PHEV use. The increasing number of PHEVs is expected to add an additional 18% load to existing power grids and this may impact the grid reliability due to less predictable overloads [3], [4]. In addition, the vehicles' relatively short driving range and their long battery charging time, compared to gasoline vehicles, need to be improved. At this stage, PHEV charging stations are an essential factor for the success of PHEVs, along with their performance improvement [6], [7],

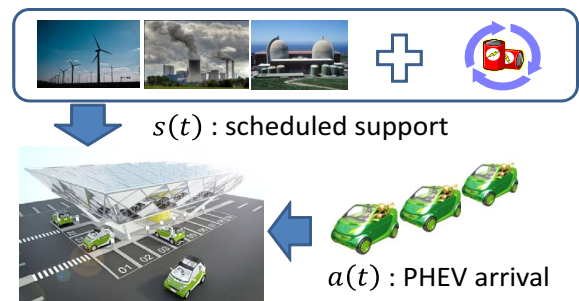


Fig. 1. An overview of PHEV charging station: Incoming vehicles ( $a(t)$ ) are serviced by electricity support ( $s(t)$ ) directly from power grids or a large capacity battery. Also, there is a space limitation for vehicles waiting at stations [5].

[8]. They are required to satisfy both the stability of power grids and to offer a reasonable QoS (Quality of Service) to customers.

This paper proposes an efficient operational framework for multiple charging stations, in the sense of the throughput of stations and the QoS offered to customers. We consider two reasons that affect these performance metrics: First, power grids establish their *generation scheduling* based on demand expectation [9], [10], [11]. For charging stations, this troubles to a time-varying electricity regulation during demand peak time. Hence, the charging capability of stations can be limited and the QoS and throughput are also affected by it.

Second, *the behavior of customers* has a high impact on the performance. In general, charging stations provide different service levels due to their facility size (e.g., the number of charging plugs or waiting spaces). Also, the charging speed of plugs may vary due to generation scheduling. As a result, the customer behavior affects not only their QoS (e.g., expected time to charge), but also the throughput of the stations.

Under these constraints, our objective is to introduce a simple notification system for customers to induce QoS maximization behavior. This notification system could be implemented through TPEG (Transport Protocol Experts Groups), which allows the real time information delivery to PHEVs [12] (e.g., real traffic information service in GPS) or smart-phone applications either based on 3G network or Internet [13].

In our analysis, we model  $n$  PHEV charging stations as a multi-queue system, where each station corresponds to a single queue. From Fig. 1, the vehicle backlog dynamics at station  $i$

( $Q_i(t)$ ) are simply described by the following equation:

$$Q_i(t+1) = \max[Q_i(t) - s_i(t), 0] + a_i(t), \quad i = 1, \dots, n \quad (1)$$

where  $s_i(t)$  is the amount of electricity supplied by the grid to the station and  $a_i(t)$  is the number of PHEV arrivals to station  $i$  at time  $t$ .

Eq. (1) includes a basic supply and demand relationship. In smart-grids, this supply and demand control is traditionally used either to maximize profit or to guarantee the system reliability. For example, support planning methods under anticipated (or reported) demands are found in [14], [15] and [16], [17], [18] study a demand adjustment based on optimization, reinforcement learning or dynamic programming.

In our framework, we assume that the support  $s_i(t)$ , which guarantees the stability of power grids, is given for stations by the electricity planning mechanism. We study a demand control method (i.e., the station visiting pattern of PHEVs) to maximize the performance under this scheduled support.

In contrast to previous smart-grid examples, there exist issues caused by the presence of multiple charging stations:

- **Station Selection:** To receive service, PHEVs are required to select a charging station. This is different from the direct transaction between supplier and customer, as customer QoS and station throughput are affected by their station selections.
- **PHEV Controllability:** Customer behaviors are *spontaneous*. For example, a customer can enter any neighboring charging stations and it is hard for stations to refuse service. Therefore, implementing a notification system without enforcing behavior is not effective to improve performance.

We proceed with a two level investigation of these issues. In our framework, we first consider customer behavior which improves QoS and throughput and we suggest a control algorithm corresponding to this behavior. Then, we test several price control methods to induce customer behaviors into the desired pattern. This is to overcome the controllability issue by giving incentives (or penalties) to customers.

The remainder of this paper is organized as follows: In section 2, we describe the problem setting of multiple PHEV charging stations and define our objectives. Section 3 derives an optimal PHEV allocation policy which satisfies our objectives and we propose its corresponding control algorithm. Then, we provide price control methods which mimic the algorithm at charging stations in section 4. Several test results to validate our analysis and algorithms are given in section 5. After that, we conclude this paper with a summary and discussion.

## II. PROBLEM DESCRIPTION

We consider an urban area, where multiple charging stations exist in the neighborhood of PHEVs, and define  $\mathcal{N}$  as the station set, where  $|\mathcal{N}| = n$ . Each station corresponds to a single queue structure as shown in Fig. 2 (i.e.,  $n$  queue system). We set  $Q_i(t)$  as the size of queue  $i$  at time  $t$ , where  $i \in \mathcal{N}$ , and its dynamics follow eq. (1).

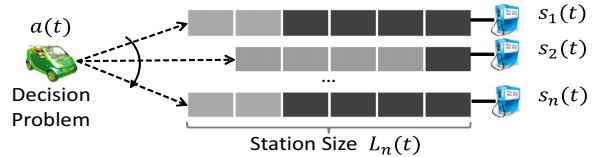


Fig. 2. Multi-Station Framework: We model  $n$  charging stations as  $n$  M/M/1 queue system. We assume that service is regulated by support scheduling, and we consider the decision problem of customers maximizing their performance.

For customers, the charging takes an exponential amount of time with rate  $\mu_i$ , where  $i = \{1, \dots, n\}$ . Further, we consider that the occurrence of PHEV charging events follows a Poisson process with rate  $\lambda$ . From the assumption that  $n$  stations are located in the neighborhood and by Poisson thinning property, the arrival process at each station is also Poisson with rate  $\lambda_i$ . Under these conditions, each queue in the system is a M/M/1 queue and it suffices to analyze their queue dynamics by considering their input and output rates.

For convenience, we define vectors  $\vec{\lambda}$  and  $\vec{\mu}$  whose elements denote the rate of PHEV arrival ( $\lambda_i$ ) and station service ( $\mu_i$ ), respectively. Customers enter one of the stations after the charging station selection and this lets us consider a constraint such that  $\sum_{i=1}^n \lambda_i$  is equal to  $\lambda$ .

The service at stations is work-conserving (i.e., each station always keeps servicing if there is a waiting vehicle) and the service rate vector, which guarantees the power grid stability, is pre-defined (i.e., deterministic) by the electricity planning mechanism. Each station can hold a limited number of waiting PHEVs due to facility differences. Similarly, we set a station size vector  $\vec{L}$  and each element  $L_i$  denotes the station capacity in terms of PHEVs.

When  $\vec{\mu}(t)$  (i.e., the electricity scheduling profile) and  $\vec{L}$  are given, we consider the control policy of vehicle allocation vector  $\vec{\lambda}$  which increases the QoS of customers and the throughput of stations. Then, we relate this to the charging price control at stations, in order to induce spontaneous customer behavior toward the objective satisfying  $\vec{\lambda}$ .

## III. VEHICLE ALLOCATION ANALYSIS

Our first objective is to study a load balancing policy to optimize vehicle allocation. This includes both minimizing the waiting time of customers and preventing the overflow of a station's waiting size. We propose a vehicle allocation algorithm which satisfies these objectives in this section.

### A. Optimized Load Balancing

As all queues are work-conserving, they need to be non empty all the time to improve the station throughput. At the same time, customer balancing is required under the given service rate  $\vec{\mu}$ . From the stationary distribution of M/M/1 queue, we note that the mean queue size ( $E[N]$ ) at each station is computed by  $E[N_i] = \frac{\mu_i}{\mu_i - \lambda_i}$ . This is directly related to the waiting time of customers in a queue. By Little's law,  $E[N_i]$  is proportional to the waiting time. For this reason, we

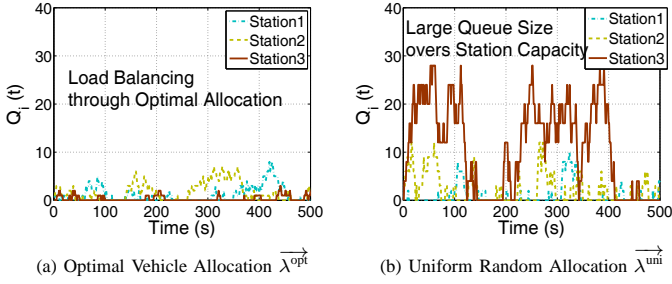


Fig. 3. The effect of optimal allocation: For  $t \in (0, 500]$ , (a) and (b) express the dynamics of the number of vehicles waiting in the three charging stations.

	Optimal Allocation	Uniform Random
Mean Queue size	3.307	15.124
Throughput	6337	6343

TABLE I  
MEAN GLOBAL QUEUE SIZE AND THROUGHPUT DURING 10,000 s.

consider the following optimization problem which minimizes the global queue size  $\sum_{i \in \mathcal{N}} E[N_i]$ :

$$\underset{\vec{\lambda}}{\text{minimize}} \quad \sum_{i=1}^n \frac{\mu_i}{\mu_i - \lambda_i} \quad (2)$$

$$\text{subject to} \quad \sum_{i=1}^n \lambda_i = \lambda \quad (3)$$

$$\mu_i - \lambda_i > 0 \quad (4)$$

$$\mu_i > 0, \lambda_i > 0 \quad (5)$$

This finds the vector  $\vec{\lambda}$  which minimizes the global number of waiting customers. The value  $\lambda$  is the occurrence rate of PHEV charging events and each subjective condition describes the load balancing through poisson thinning, stability, positive arrival and departure rates, respectively.

The solution vector  $\vec{\lambda}^{\text{opt}}$  of this problem is given by:

$$\lambda_i^{\text{opt}} = \frac{\lambda + \sum_{j=1}^n (\sqrt{\mu_i \mu_j} - \mu_j)}{\sum_{j=1}^n \sqrt{\frac{\mu_j}{\mu_i}}}, \text{ where } i = \{1, \dots, n\} \quad (6)$$

Procedures to find the solution (6) are given in Appendix A.

We emphasize the necessity and importance of the appropriate vehicle allocation policy through a simple 3 station example. To show the effectiveness of  $\vec{\lambda}^{\text{opt}}$ , we compare the queue dynamics between the optimal allocation and a uniformly random policy ( $\vec{\lambda}^{\text{uni}}$ ). The uniformly random policy allocates PHEVs to stations with equal probability  $\frac{1}{n}$  and this is suitable whenever customers do not receive any information from the stations. For three stations, we set  $\vec{\mu} = [1/2, 1/3, 1/4]$  and  $\lambda = 1$ . The optimal allocation vector  $\vec{\lambda}^{\text{opt}}$  becomes  $\lambda[0.4670, 0.3063, 0.2267]$  by using (6) and  $\lambda_i^{\text{uni}} = \frac{1}{3}\lambda$  for  $i = \{1, 2, 3\}$ . For each incoming vehicle, we proceed with a probabilistic station selection and the probability to select station  $i$  is set to  $p_i = \lambda_i^{\text{strategy}}/\lambda$  (i.e., normalization).

Initially, all stations are empty and we test each strategy for 10,000 s. Fig. 3 plots the queue size dynamics for the first

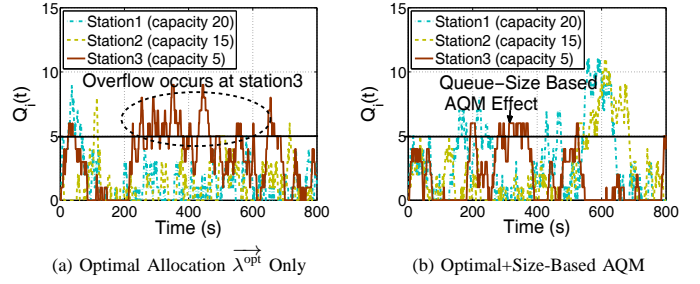


Fig. 4. The effect of size-based AQM under optimal allocation: For  $t \in (0, 800]$ , (a) and (b) show the station size dynamics under optimal allocation policy (6) only and Alg. 1 which considers  $L$ , respectively.

500 s and Table. I depicts the mean global queue size (i.e.,  $\sum_{i=1}^3 E[N_i]$ ) and throughput, which measures the number of processed vehicles in  $t \in (0, 10000]$ . From Fig. 3(a) and (b), we observe the load balancing capability of  $\vec{\lambda}^{\text{opt}}$ . Minimizing the global queue size ( $\sum_{i \in \mathcal{N}} E[N_i]$ ) is also effective to reduce the size of local queues ( $E[N_i]$ ). To reduce the global queue size, the solution (6) produces a higher allocation probability for the stations with the higher processing (charging) capability. This is an intuitive approach, but the solution is not simply proportional to  $\vec{\mu}$ . Also, Table I indicates that the allocation  $\vec{\lambda}^{\text{opt}}$  achieves almost 80% reduction in the queue size without losing throughput performance.

### B. Station Size Limitation and Vehicle Allocation Algorithm

The vehicle allocation vector  $\vec{\lambda}^{\text{opt}}$  gives a load balancing capability and this supports a lower waiting time for customers while charging their PHEVs. Now, we consider the station's capacity constraint. This is included in the size vector  $\vec{L}$ , where an element  $L_i$  indicates the size capacity of station  $i$ . First, the solution  $\vec{\lambda}^{\text{opt}}$  assumes that the size of stations is infinite. However, the computed mean number of waiting customers at each station under the allocation (i.e.,  $E[N_i] = \frac{\mu_i}{\mu_i - \lambda_i^{\text{opt}}}$ ) can be over the capacity of stations (i.e.,  $E[N_i] > L_i$  for some  $i \in \mathcal{N}$ ).

Second, the optimal allocation requires a stability condition on local queues. During peak times, the incoming PHEV rate can be temporarily higher than service rate (i.e.,  $\lambda_i^{\text{opt}} > \mu_i$ ) and this leads to an increase of the local queue size.

In the previous example, suppose the station size vector is  $\vec{L} = [20, 15, 5]$ . Then, we observe that overflows appear at station 3 in Fig. 3(b). Although the allocation  $\vec{\lambda}^{\text{opt}}$  prevents the overflows as shown in Fig. 3(a), this still occurs under the optimal allocation. Consider that the customer arrival is increased by 30% during a demand peak time. Under the same station setting, we adjust  $\lambda$  into 1.3. Fig. 4(a) plots the queue-size dynamics and we again see overflows at station 3.

To mitigate this temporal station capacity overflow, we utilize a size-based active queue management (AQM). We set a congestion indicator  $c_i(t)$  as shown below:

$$c_i(t) = \mathbf{1}_{\{Q_i(t) > L_i\}}, \text{ where } i \in \mathcal{N} \quad (7)$$

The purpose of this setting is to exclude stations experiencing congestion in the computation of the optimal allocation (6). The following Alg. 1 describes this:

---

**Algorithm 1** PHEV Allocation Control by using AQM

---

**Require:**  $\lambda$ ,  $\vec{\mu}(t)$  and  $\vec{c}(t)$  with size  $|\mathcal{N}|$   
**for**  $i = 1 \rightarrow |\mathcal{N}|$  **do**  
  **if**  $c_i(t) = 1$  **then**  
     $\mu_i(t) \leftarrow 0$  (Exclude Station  $i$ )  
  **end if**  
**end for**  
 $\lambda^{\text{opt}}(t+1) \leftarrow \frac{\lambda + \sum_{j=1}^{|\mathcal{N}|} (\sqrt{\mu_i \mu_j} - \mu_j)}{\sum_{j=1}^{|\mathcal{N}|} \sqrt{\frac{\mu_j}{\mu_i}}}$

---

By setting  $\mu_i = 0$  for the station  $i$  experiencing congestion, Alg. 1 induces  $\lambda_i^{\text{opt}} = 0$ . In the computation of  $\vec{\lambda}^{\text{opt}}$  at the next time step, this makes an optimal vehicle allocation among non-overflowing stations. We compare this AQM added strategy, which accounts for the capacity limitation  $\vec{L}$ , with the optimal allocation only case in Fig. 4(b). In contrast to Fig. 4(a), overflows at station 3 are now controlled and we see that the overflow vehicles are balanced to station 1 and 2.

#### IV. CUSTOMER CONTROL BY USING PRICE MATCHING

Until now, the allocation policy  $\vec{\lambda}^{\text{opt}}$  to maximize throughput and QoS has been investigated while assuming that the behavior of customers is controllable. However, in reality, it is hard to expect from customers to follow this policy even if they are aware of the optimal allocation. For this reason, we give an incentive to customers by differentiating the charging price at stations under the assumption that customers generally prefer to select a station which supports a lower charging price. By using a price control, we propose methods which make the PHEV allocation mimic Alg. 1.

We set common conditions in our price matching methods. The price update at stations occurs periodically with duration  $T$  and the price range varies within  $(p_{\min}, p_{\max})$  in a day. Also, stations measure the average input  $(\bar{\lambda}_i)$  and output rate  $(\bar{\mu}_i)$  every  $T$  units of time, in order to estimate their traffic status variation. The value  $\bar{\lambda}$  implies the estimated summation of PHEV arrivals during  $T$  (i.e.,  $\bar{\lambda} = \sum_{i \in \mathcal{N}} \bar{\lambda}_i$ ) [19].

##### A. Method 1: Utilizing a Price Sensitivity Function

First, we consider the case when the price sensitivity of customers is known. In general, this can be any decreasing and differentiable function, and a more sophisticated form can be attained by using customer surveys or reinforcement learning while operating the framework [18].

Suppose that a probability function  $f$  exists for the price sensitivity of customers. When the function satisfies an one-to-one correspondence, there always exists its inverse form. This provides an exact price setting at stations to induce relevant customer behaviors:

$$q_i = f(p_i) \leftrightarrow p_i = f^{-1}(q_i), \text{ for all } i \in \mathcal{N} \quad (8)$$

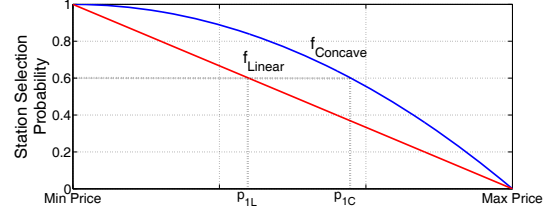


Fig. 5. The price sensitivity function  $f$ : When this is known to charging stations and satisfies an one-to-one correspondence, the direct price matching to induce a desired customer behavior is available by using an inverse function  $f^{-1}$ . We consider two sensitivity types for our tests.

When stations update their price at time  $t_k$ , they have an estimation for customer arrival rate  $\bar{\lambda}_i$  for a period  $T$  (i.e., a time window  $(t_k - T, t_k)$ ) and Alg. 1 provides the optimized PHEV allocation vector  $\vec{\lambda}^{\text{opt}}$  based on these measurements. Utilizing a normalization  $\lambda_i^{\text{opt}}/\bar{\lambda}$  makes this into a weight vector.

For the price decision for the upcoming duration  $(t_k, t_k + T]$ , we convert this weight vector to the station price vector  $\vec{P}_{(t_k, t_k + T]}$  by using (8):

$$\vec{P}_{(t_k, t_k + T]} = [f^{-1}(\frac{\bar{\lambda}_1}{\bar{\lambda}}), \dots, f^{-1}(\frac{\bar{\lambda}_{|\mathcal{N}|}}{\bar{\lambda}})] \quad (9)$$

This price marking induces a customer behavior appropriate for the optimal allocation. In addition, the effect of overflow relaxation is already included in it. When an overflow (i.e.,  $c_i(t) = 1$ ) occurs, Alg. 1 excludes the station in the  $\vec{\lambda}^{\text{opt}}$  computation, by setting  $\lambda_i^{\text{opt}} = 0$ . In (9), this corresponds to the highest price due to the decreasing  $f$  and a customer selection for that station decreases significantly in the next  $T$  duration.

We test this approach under linear and concave functions. Both include the decreasing customer preference to the price increment and, especially, the latter concave function implies that the customer selection becomes more sensitive to the price increase. We also compare the differences when the congestion notification  $c(t)$  is used or not under this price matching.

##### B. Method 2: Regression Based Price Control

We suggest a regression method for adjusting the charging price of stations based on a simple first order auto regressive (AR-1) model. Utilizing higher order models or Additive Increase and Multiple Decrease (AIMD), similar to that used in Internet congestion control [20], will improve the performance in the price adjustment speed. However, for the scope of this paper, we focus on showing that the charging price adjustment is available even if the customer behavior function  $f$  is unknown. To simplify our treatment, the price update framework is considered as a discrete time system. Each time-slot duration is  $T$  and stations share the averaged values  $\bar{\lambda}_i$  and  $\bar{\mu}_i$  at each price update instance for all  $i \in \mathcal{N}$ .

We proceed with the greedy price control of stations by using the rate difference between the optimal  $\lambda_i^{\text{opt}}(t)$  and measurement  $\bar{\lambda}_i(t)$ . At time  $t$ , we set this difference to  $d_i(t)$ :

$$d_i(t) = \bar{\lambda}_i(t) - \lambda_i^{\text{opt}}(t), \text{ where } i \in \mathcal{N} \quad (10)$$

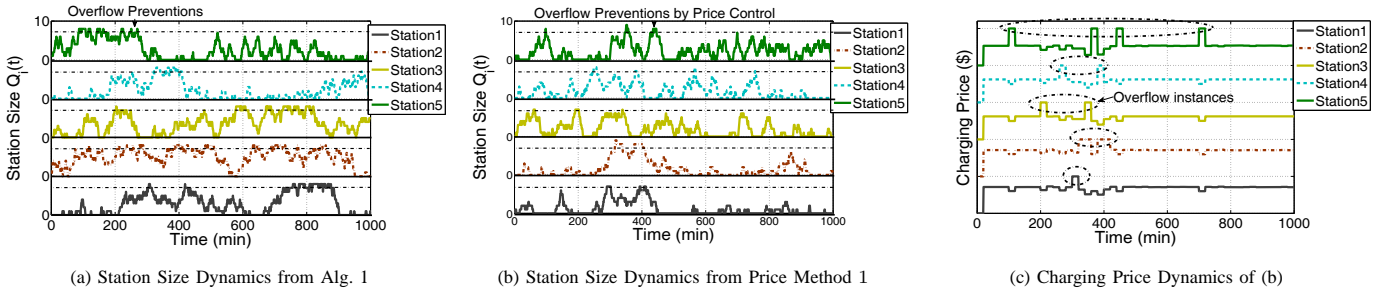


Fig. 6. Station size dynamics comparison between Alg. 1 and price method 1 under linear  $f_1$ : The tick size of Y-axis is 10 in (a) and (b).

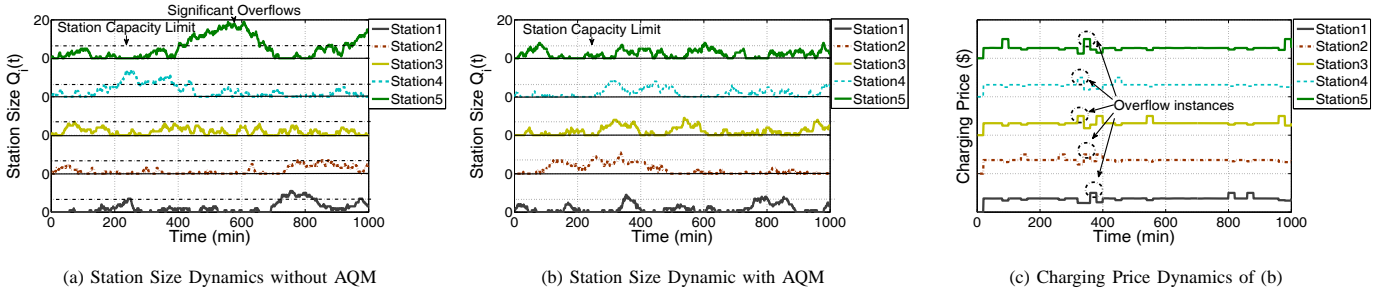


Fig. 7. The station size variation depending on AQM when the price method 1 with concave  $f_2$  is used: The tick size of Y-axis is 20 in (a) and (b).

The occurrence of PHEV charging events has a temporal correlation (i.e., the steep increase or decrease of the summed station visiting rate  $\bar{\lambda}$  rarely occurs). Under this,  $\bar{\lambda}^{\text{opt}}$  defines an objective rate to maximize performance. Thus, a positive  $d_i(t)$  means that more vehicles than optimal are entering into station  $i$ , meaning that it is required to decrease the input rate. In addition, the opposite case also holds. By controlling the price of stations, we posit the regression model:

$$p_i(t+1) = p_i(t) + \gamma d_i(t), \text{ where } i \in \mathcal{N} \quad (11)$$

Under the assumption that customers select stations inverse-proportionally to their charging price, this simple regression would incur a price convergence to  $p_i^*$ , where the difference  $d_i(t)$  becomes 0. Note that (11) always works into the direction that  $d_i(t)$  decreases even if time-varying changes occur in  $\bar{\lambda}$  and  $\bar{\mu}$ . The issue is the convergence speed (i.e., whether a fast customer response is possible through price adjustments), which is related to the parameter  $\gamma$  (Note, higher order regressions and AIMD can relax this even under their occurrences).

We also expect that the overflow relaxation can be attained by using (11). As Alg. 1 allocates  $\lambda^{\text{opt}}$  to 0 for congesting experiencing charging stations, the additive term  $\gamma d_i(t)$  becomes a maximum under station overflow, and this gives a clear price increase, compared with non-congestion experiencing stations.

We show that this regression model can adjust charging prices to mimic Alg. 1 even if the price sensitivity of customers is unknown to charging stations. Also, we compare the price convergence behavior with a varying speed parameter  $\gamma$ .

## V. TEST CASES AND DISCUSSIONS

The service rate vector  $\bar{\mu}$  is originally time-varying according to the support scheduling of power grids. However, we first fix the service rate vector  $\bar{\mu}$  to test the effectiveness of our

price control methods. In particular, we want to see whether they are capable of attaining the effect of Alg. 1 by controlling prices. After that, we show test results in the case where the scheduled electricity support plan is time-varying.

### A. Price Adjustment Method Tests

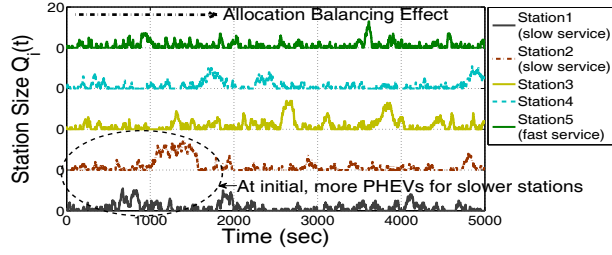
1) *Method 1 Test:* Here, the price sensitivity of customers is known. We set  $|\mathcal{N}| = 5$ ,  $\bar{\mu} = [0.2, 0.2, 0.25, 0.25, 0.3]$  and  $L_i = 7$ , where  $i \in \mathcal{N}$ , in common. The price update of stations occurs at every  $T = 20$  (min) with synchronization. At each price update instance  $t_k$ , stations share the estimated average rate  $\bar{\lambda}_i(t_k - T, t_k]$ ,  $\bar{\mu}_i(t_k - T, t_k]$  and the congestion status  $c_i(t_k)$ . Then, the optimal PHEV allocation  $\bar{\lambda}$  is computed by using Alg. 1. The price range  $(p_{\min}, p_{\max})$  is set to  $(6, 15)$  based on 200 (miles/charging) and 0.03 (dollars/mile) [3]. We use two types of customer behavior functions  $f_1$  and  $f_2$ , which are linear and concave, respectively:

$$f_1(p) = -\frac{1}{p_{\max} - p_{\min}}p + \frac{p_{\max}}{p_{\max} - p_{\min}}, f_2(p) = 1 - \left(\frac{p}{p_{\max}}\right)^2 \quad (12)$$

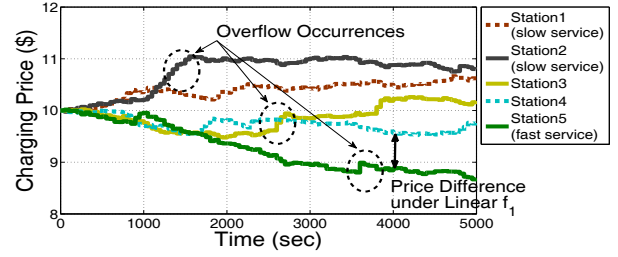
The shape of these functions is shown in Fig. 5.

We first test whether the price control by (9) is equally effective as the direct rate control of Alg. 1. Under the use of *linear* customer function  $f_1$  and PHEV arrival rate  $\lambda = 1.5$ , Fig. 6(a) and (b) plot the station dynamics for 1,000 mins by using Alg. 1 and price control method 1, respectively.

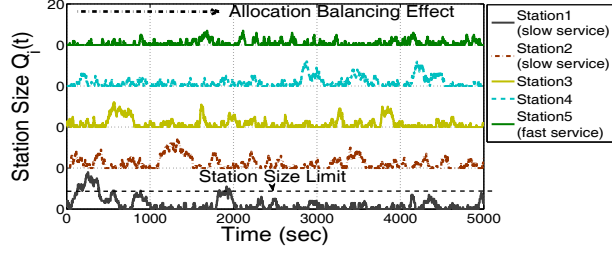
For both cases, more vehicles are allocated to the faster processing capable stations (i.e., those with higher  $\mu$ ) and station overflows are relaxed by the size-based AQM. In contrast to Alg. 1 which suffers from consistent overflows once when occur, congestions appear as peaks under this price control mechanism. This can be explained by the update period  $T$ . Once a high price is set due to congestion, the price is kept



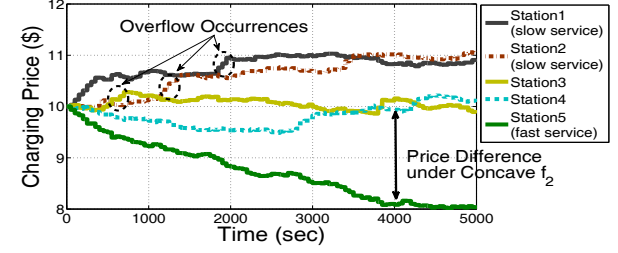
(a) Station Size Dynamics when Customer Behavior Follows the Linear  $f_1$



(b) Charging Price Dynamics when Customer Behavior Follows the Linear  $f_1$



(c) Station Size Dynamics when Customer Behavior Follows the Concave  $f_2$



(d) Charging Price Dynamics when Customer Behavior Follows the Concave  $f_2$

Fig. 8. Price method 2 test results: In all results, the customer behavior function  $f_1$  and  $f_2$  are unknown to stations. (a) and (b) plot the dynamics under the linear  $f_1$ . (c) and (d) are dynamics under the concave  $f_2$ . Two price sensitivity functions are shown in Fig. 5 and the parameter  $\gamma$  in (11) is set to 0.5.

until the next price update instance. Thus, our price method is more effective to reduce station overflows. Fig. 6(c) plots the dynamic price matching under method 1. In there, we see price peaks at stations when overflows occur and these match to the instances of size overflows shown in Fig. 6(b).

Fig. 7(a) and (b) show the station size dynamics when the behavior of customers follows the *concave* function  $f_2$  with  $\lambda = 2$  (i.e., the occurrence of PHEV charging events is increased by 33.3%). These comparisons show the effectiveness of size-based AQM. In Fig. 7(a), where only the optimal PHEV allocation (6) is used without AQM, we see station overflows under this increased PHEV charging event rate. In contrast, these overflows disappear and the amount of overflows are redistributed to other non-congesting stations in Fig. 7(b), where AQM is added to the optimal allocation. The dynamic price adjustment of this is shown in Fig. 7(c).

2) *Method 2 Test*: We test the rate difference based regression (11) with  $\gamma = 0.5$ . Results are plotted in Fig. 8. Here, the customer behavior is decided by either  $f_1$  or  $f_2$  and it is unknown to charging stations when they decide price updates.

We use the same service vector  $\vec{\mu}$  and price range  $(p_{\min}, p_{\max})$ , and the charging price for stations is set to \$10 at initial. In contrast to method 1 tests, stations update their price in every minute. This fast update is necessary, as the price variation at each update is limited by the small factor  $\gamma d_i(t)$  in (11). Fig 8(a) and (b) shows the dynamics under the linear customer  $f_1$  and Fig 8(c) and (d) are under the concave customer  $f_2$ . The following major findings are from these experiments:

- **Autonomous Price Adjustment**: Although the customer behavior function  $f$  is unknown to the stations, there occurs a price differentiation among charging stations. From the price dynamics Fig. 8(b) and (d), we observe

that price stabilization is achieved by regression updates. These price differentiations autonomously capture the *unknown* customer behavior. For example, at  $t=4,000$ , the price gap between station 1 and 2 appears larger under the concave  $f_2$  (Fig. 8(d)), than under the linear  $f_1$  (Fig. 8(b)). We note that a bigger price reduction is required under  $f_2$  to induce the same optimal behavior  $\lambda^{\text{opt}}$ , as customers are more sensitive to the price increment under concave functions (see Fig. 5).

- **Load Balancing**: Initially, the price method 2 is the same as that of uniform PHEV allocation policy since there is no price differentiation among stations. Thus, more PHEVs are stuck at slower service stations (i.e., those with smaller  $\mu$ ) at the early phase in both Fig. 8(a) and (c). We observe that these imbalances disappear as the price adjustment through the regression (11) evolves.
- **Overflow Relaxation**: In the price dynamics Fig. 8(b) and (d), there appear instances where the variation of charging prices has a steep and continuous increase. These match overflow occurrences as shown in Fig. 8(a) and (c). This verifies our expectation that the price variation  $\gamma d_i(t)$  is maximized at updates under overflows and shows its effectiveness to relax overflows.

Method 2 requires an initial warm-up phase to induce a price stabilization and this highly depends on the regression parameter  $\gamma$ . For this reason, we plot the price variations for station 1 and 5 with varying  $\gamma$  in Fig. 10. Although overshoot degrees are different, we still observe that the price converges to  $p_1^*$  and  $p_5^*$ , respectively, regardless of  $\gamma$ .

### B. Tests under Electricity Support Regulation

We differentiate the service rate of charging stations according to the electricity support scheduling. Fig. 9(a) shows the

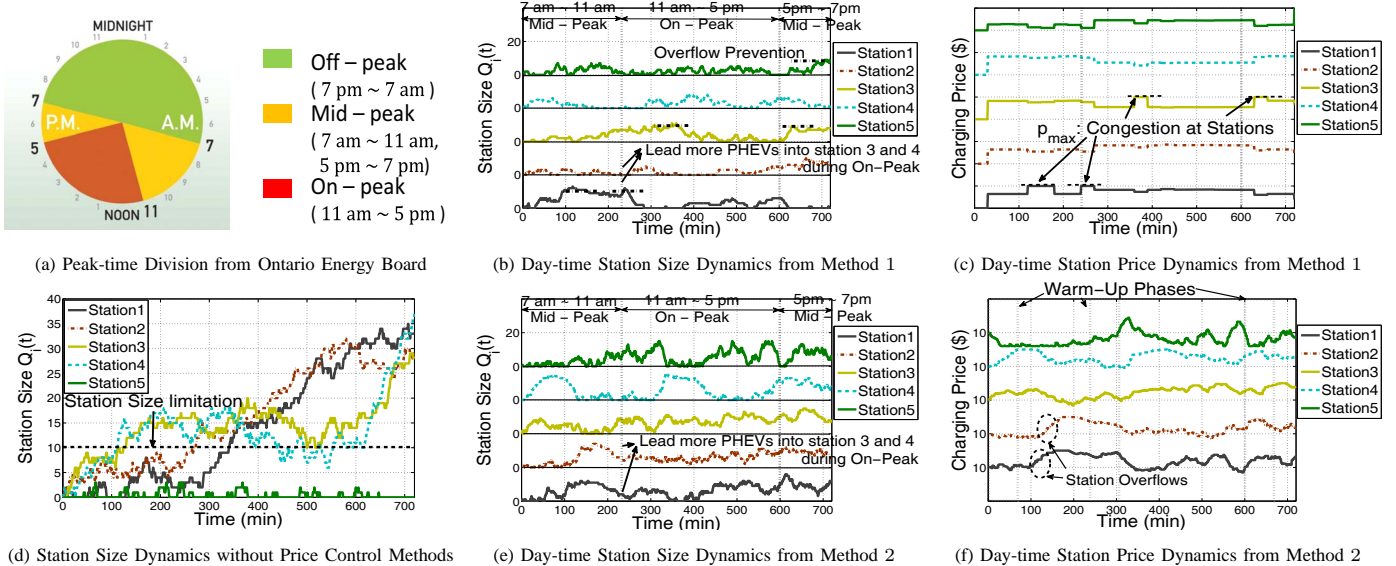


Fig. 9. Test results under electric support regulations: During a day-time the service at charging stations is regulated by (a) and eq. (13). (d) plots the station dynamics without price control methods. We compare the result with the dynamics under method 1 ((b) and (c)) and method 2 ((e) and (f)).

peak-time division from Ontario Energy Board during summer time (May 1 ~ Oct.31) [11]. We perform day-time simulations (7 am~7 pm) where both an on-peak and a mid-peak exist. We set 5 neighboring charging stations and their service rates to be regulated by the following  $\vec{\mu}_{\text{Mid-Peak}}$  and  $\vec{\mu}_{\text{On-Peak}}$ :

$$\begin{aligned} \vec{\mu}_{\text{Mid-Peak}} &= [0.2, 0.2, 0.1, 0.1, 0.4] \\ \vec{\mu}_{\text{On-Peak}} &= [0.1, 0.1, 0.25, 0.25, 0.3] \end{aligned} \quad (13)$$

The rate of PHEV charging events is also time-varying. We set  $\lambda = 3$  for commute times (7 am~8 am, 5 pm~6 pm) and a lunch time (12 pm~1 pm). All other periods have  $\lambda = 2$ . The price range is (6, 15) and the size  $L_i$  is 10 for stations.

First, we plot the station backlog dynamics under the uniformly random allocation policy in Fig 9(d). This indicates the situation where there is no PHEV control framework. Under this, we observe severe overflows at station 1~4.

Fig. 9(b) is the station dynamics under the price control method 1 with the customer behavior function  $f_1$  and  $T = 30$  (min). The horizontal dash lines are overflow occurrence points and we observe that those are well alleviated through price control and relaxed in a short time. Further, we observe the dynamic PHEV allocation according to the support scheduling.

Station 3 and 4 start providing the faster service than station 1 and 2 during on-peak times from the electricity regulation (13). In Fig. 9(b), it can be that the customers behavior is adjusted to the support regulation by the price control shown in Fig. 9(c).

Fig. 9(e) and (f) are test results for the price method 2 when  $\gamma = 1.5$  and  $T = 5$  (min). In comparison to Fig. 9(d), method 2 shows adequate overflow relaxations. We also see the dynamic allocation adjustment to the time-varying support by observing the variation of station dynamics during peak-times. In contrast to the method 1, there appear warm-up phases, expressed as rectangular areas, to stabilize the charging price as shown in Fig. 9(f). Also, method 2 takes a little bit more time to relax overflows. These are due to the limited price variation at each update that comes from the parameter  $\gamma$ .

We also measure the total throughput of stations during simulations. Under the price control method 1 and 2, charging stations provide a service for 601 and 546 PHEVs, respectively. When there is no price control, the number of serviced vehicles is 532. This implies that the proposed price control methods are beneficial not only for customers, but also for the throughput of stations.

## VI. CONCLUSION

In this paper, we proposed a PHEV charging station framework to satisfy both the QoS of customers and the power-grid stability. We started from the reasoning why this framework is necessary in smart-grid communities. Under the electricity regulation of PHEV stations which is to guarantee the stability of power systems, we showed by examples that QoS and throughput can be very different according to the existence of PHEV allocation policy.

We performed a two-stage investigation to build our framework. Our initial objective was to find an optimal customer

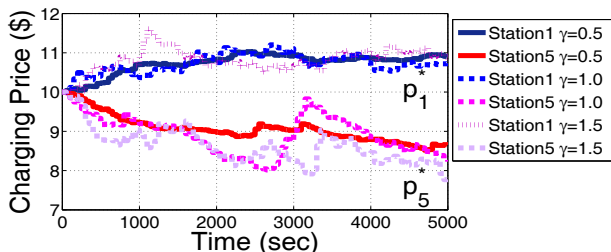


Fig. 10. The effect of regression parameter  $\gamma$  in method 2 price dynamics.

behavior to maximize their QoS and to prevent station overflows. We derived an optimal solution which satisfies the first objective and the second objective is resolved by utilizing a size-based AQM. Based on these, we proposed a PHEV allocation algorithm.

Subsequently, we related this algorithm to price control methods. This is because customers are allowed to select charging stations spontaneously, even if the optimal solution is known. A price control represents an effective way to offset their behavior by providing incentives (or penalties). We suggested two price matching methods which are distinguished by whether the price sensitivity of customers is known a priori or not. For both cases, we explained the reasoning of our price matching and provided test results to validate them. Finally, under the scheduled electricity support (i.e., time-varying regulation), these methods were tested and we showed their feasibility to satisfy our objectives.

#### APPENDIX A: PROCEDURES TO COMPUTE THE OPTIMAL SOLUTION (6)

We show this optimization is convex. First, all subject functions are linear. For the objective functions, suppose  $g(\lambda) = \frac{\mu}{\mu-\lambda}$ . Then,  $g''(\lambda) > 0$  for all  $\lambda$  under the stability condition (4). As the summation of convex functions is also convex, the objective function is also convex.

Now, consider its Lagrange dual  $L(\vec{\lambda}, u)$ :

$$L(\vec{\lambda}, u) = \sum_{i=1}^n \frac{\mu_i}{\mu_i - \lambda_i} + u \left( \sum_{i=1}^n \lambda_i - \lambda \right) \quad (14)$$

When the problem is convex, this is a Wolfe dual problem so that it is minimized when  $\nabla L(\vec{\lambda}, u) = 0$  is satisfied. We use a mathematical induction to obtain  $\lambda^{\text{opt}}$  for a general  $n$  station case.

Suppose  $n = 2$  and find  $\vec{\lambda}^{\text{opt}} = [\lambda_1, \lambda_2]$ . Then,  $\nabla L(\vec{\lambda}, u) = \left[ \frac{\partial L(\vec{\lambda}, u)}{\partial \lambda_1}, \frac{\partial L(\vec{\lambda}, u)}{\partial \lambda_2}, \frac{\partial L(\vec{\lambda}, u)}{\partial u} \right]$  becomes:

$$\frac{\partial L(\vec{\lambda}, u)}{\partial \lambda_1} = \frac{\mu_1}{(\mu_1 - \lambda_1)^2} + u \quad (15)$$

$$\frac{\partial L(\vec{\lambda}, u)}{\partial \lambda_2} = \frac{\mu_2}{(\mu_2 - \lambda_2)^2} + u \quad (16)$$

$$\frac{\partial L(\vec{\lambda}, u)}{\partial u} = \lambda_1 + \lambda_2 - \lambda \quad (17)$$

By setting  $\nabla L(\vec{\lambda}, u) = 0$ , we find the solution which satisfies stability (i.e.,  $\mu_i > \lambda_i$ ) and positive parameter (i.e.,  $\lambda, \mu > 0$ ) conditions. The optimal allocation  $\lambda^{\text{opt}}$  becomes:

$$[\lambda_1^{\text{opt}}, \lambda_2^{\text{opt}}] = \left[ \frac{\lambda + \sqrt{\mu_1 \mu_2} - \mu_2}{1 + \sqrt{\mu_2 / \mu_1}}, \frac{\lambda + \sqrt{\mu_1 \mu_2} - \mu_1}{1 + \sqrt{\mu_1 / \mu_2}} \right] \quad (18)$$

When  $n = l$ ,  $\nabla L(\vec{\lambda}, u) = 0$  has  $l$  equations. Assume the optimal solution  $\lambda_i^{\text{opt}}$ , where  $i = \{1, \dots, l\}$ , follows the solution  $\lambda_i^{\text{opt}} = \frac{\lambda + \sum_{j=1}^n (\sqrt{\mu_i \mu_j} - \mu_j)}{\sum_{j=1}^n \sqrt{\frac{\mu_j}{\mu_i}}}$ , where  $i = \{1, \dots, l\}$ .

Now, consider the  $\nabla L(\vec{\lambda}, u) = 0$  when  $n = l + 1$ . For the first  $l$  equations, they have a form of (15) or (16):

$$\frac{\partial L(\vec{\lambda}, u)}{\partial \lambda_i} = \frac{\mu_i}{(\mu_i - \lambda_i)^2} + u, \text{ where } i \in \{1, \dots, l\} \quad (19)$$

Select any  $m^{\text{th}}$  equation among them and eliminate  $u$  in all other  $l - 2$  equations by substituting the  $m^{\text{th}}$  equation. This induces the following  $l - 2$  equations.

$$\lambda_i = \mu_i \pm (\mu_m - \lambda_i) \sqrt{\lambda_i / \lambda_m}, \text{ where } i \in \{1, \dots, l\} \setminus m \quad (20)$$

Now, change the form of  $\sum_{i=1}^{l+1} \lambda_i = \lambda$  (i.e., the last gradient element of  $L$ ) into  $\sum_{i \in \mathcal{N} \setminus \{m\}} \lambda_i + \lambda_m = \lambda$ . Putting this into (20) gives the full solution of (6) when  $n = l + 1$ .

#### REFERENCES

- [1] D. Lemoine, D. Kammen, and A. Farrell, "An innovation and policy agenda for commercially competitive plug-in hybrid electric vehicles," *Environmental Research Letters*, vol. 3, p. 014003, 2008.
- [2] M. Duvall, E. Knipping, M. Alexander, L. Tonachel, and C. Clark, "Environmental assessment of plug-in hybrid electric vehicles. volume 1: Nationwide greenhouse gas emissions," *Electric Power Research Institute, Palo Alto, CA*, vol. 1015325, 2007.
- [3] *The Smart Grid: An Introduction*. DOE Smart Grid Book, 2008.
- [4] S. Wirasingha, N. Schofield, and A. Emadi, "Plug-in hybrid electric vehicle developments in the us: Trends, barriers, and economic feasibility," in *Vehicle Power and Propulsion Conference*. IEEE, 2008, pp. 1–8.
- [5] "[online] <http://www.evoasis.com/services/>," EVSTAT Electric Vehicle Charging Stations.
- [6] M. Kezunovic, S. Waller, and I. Damjanovic, "Framework for studying emerging policy issues associated with phev in managing coupled power and transportation systems," in *Green Technologies Conference*. IEEE, 2010, pp. 1–8.
- [7] F. Pan, R. Bent, A. Berscheid, and D. Izraelevitz, "Locating phev exchange stations in v2g," in *Smart Grid Communications (SmartGridComm)*. IEEE, 2010, pp. 173–178.
- [8] Z. Wang, P. Liu, H. Han, C. Lu, and T. Xin, "A distribution model of electric vehicle charging station," *Applied Mechanics and Materials*, vol. 44, pp. 1543–1548, 2011.
- [9] S. Wallace and S. Fleten, "Stochastic programming models in energy," *Handbooks in operations research and management science*, 2003.
- [10] B. Danai, J. Kim, A. Cohen, V. Brandwajn, and S. Chang, "Scheduling energy and ancillary service in the new ontario electricity market," in *Power Industry Computer Applications*. IEEE, 2001, pp. 161–165.
- [11] "[online] ontario energy board," <http://www.ontarioenergyboard.ca/>.
- [12] Y. Jeong and W. Kim, "A novel tpeg application for location based service using terrestrial-dmb," *Consumer Electronics, IEEE Transactions on*, vol. 52, no. 1, pp. 281–286, 2006.
- [13] M. Weiss and D. Guinard, "Increasing energy awareness through web-enabled power outlets," in *Proceedings of the 9th International Conference on Mobile and Ubiquitous Multimedia*. ACM, 2010.
- [14] M. Neely, A. Tehrani, and A. Dimakis, "Efficient algorithms for renewable energy allocation to delay tolerant consumers," in *Smart Grid Communications (SmartGridComm)*. IEEE, 2010, pp. 549–554.
- [15] A. Papavasiliou and S. Oren, "Supplying renewable energy to deferrable loads: Algorithms and economic analysis," in *Power and Energy Society General Meeting*. IEEE, 2010, pp. 1–8.
- [16] S. Caron and G. Kesidis, "Incentive-based energy consumption scheduling algorithms for the smart grid," in *Smart Grid Communications (SmartGridComm)*. IEEE, 2010, pp. 391–396.
- [17] N. Li, L. Chen, and S. Low, "Optimal demand response based on utility maximization in power networks," in *PES General Meeting*. IEEE, 2011.
- [18] D. O'Neill, M. Levorato, A. Goldsmith, and U. Mitra, "Residential demand response using reinforcement learning," in *Smart Grid Communications (SmartGridComm)*. IEEE, 2010, pp. 409–414.
- [19] M. Kallitsis, G. Michailidis, and M. Devetsikiotis, "Measurement-based optimal resource allocation for network services with pricing differentiation," *Performance Evaluation*, vol. 66, pp. 505–523, 2009.
- [20] A. Tanenbaum and D. Wetherall, *Computer networks*. Prentice Hall Press, 2010.